PROJECT ACRONYM

CUPIDO

PROJECT TITLE

Cardio Ultraefficient nanoParticles for Inhalation of Drug prOducts

Deliverable 1.4

Functional assessment (compatibility, physic- chemical and biological stability) of FeCaP restoration and drug release

CALL ID			H2020-NMBP-2016-2017
GA No.			720834
MAIN CONTACT			**Daniele Catalucci** Email: daniele.catalucci@cnr.it
NATURE	Report (R)	DISSEMINATION LEVEL	PU
DUE DATE	30/09/2018	ACTUAL DELIVERY DATE	26/11/2018
AUTHOR(S)	Alessio Adamiano, Alessandra Marrella, Jessica Modica, and Eride Quarta		

This project has received funding from the European Union's Horizon 2020 research and innovation programme under grant agreement No 720834.

Table of Revisions

REVISION NO.	DATE	WORK PERFORMED	CONTRIBUTOR(S)
1	05/10/2018	Document preparation	Alessio Adamiano, Alessandra Marrella, and Jessica Modica
2	14/10/2018	Document revision	Daniele Catalucci
3	23/10/2018	Document revision	Alessio Adamiano
4	23/10/2018	Document revision	Eride Quarta
5	02/11/2018	Document revision	Consortium
6	16/11/2018	Document revision	CCG
7	19/11/2018	Document formatting	Jessica Pellarini
8	23/11/2018	Document revision	IPR Team

Table of Contents

Index of Figures and Tables

1. Executive summary

The program was centered on the preparation and characterization of ^{Fe}CaPs and microparticles containing ^{Fe}CaPs (dp^{Fe}CaPs). Protocols for the generation of ^{Fe}CaPs and dp^{Fe}CaPs were successfully produced, and allowed the loading for several small molecules. Physic-chemical stability has been subsequently tested for both loaded and unloaded ^{Fe}CaPs. Evaluation of drug release performance under an electromagnetic stimulation was monitored with the model drug Ibuprofen (IBU). Assays were performed within a custom device developed for mimicking the cardiovascular fluidic environment. *In vitro* functional assessments of ^{Fe}CaP and dp^{Fe}CaP dynamisms of interaction and nanoparticles internalization in cardiac cells are currently ongoing.

Key deliverable achievements:

1. Small molecule loaded in superparamagnetic nanoparticles;
2. Microparticles embedding loaded nanoparticle
3. Magnetic stimulation;
4. Physico-chemical stability;
5. Drug release.

2. Cooperation between participants

ISTEC-CNR synthesized ^{Fe}CaPs and performed all the loading experiments. According to PLU indications, aqueous suspension of ^{Fe}CaPs were produced and shipped to PLU.

CNR-IEIIT assessed the properties of ^{Fe}CaPs in function of an electromagnetic stimulation and fluidic environment. Activities were conducted in tight interaction with CNR-ISTEC and CNR-IRGB.

PLU carried out the construction of dp ^{Fe}CaPs.

CNR-IRGB is currently completing the in vitro functional assessment of dpCaPs. In addition, CNR-IRGB kept the links between the involved partners, who were periodically interacting via remote teleconferences.

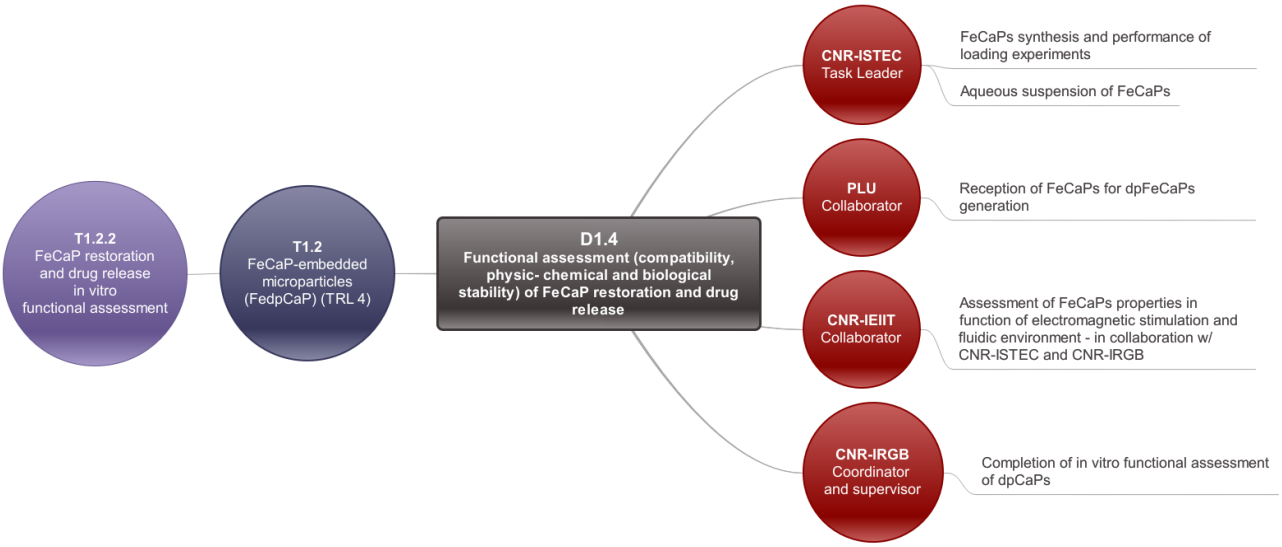

3. ^{Fe}CaP synthesis

^{Fe}CaPs displaying a typical superparamagnetic behaviour with an amount of iron of 9.7 wt% were successfully produced according to the protocol reported in a recent paper (Adamiano et al. Acta Biomaterialia, 2018). Briefly, for the synthesis of ^{Fe}CaP-001 a phosphoric acid solution (20.75 g in 300 ml H_2O) was added dropwise into a basic suspension of calcium hydroxide $Ca(OH)_2$, (23.40 g in 400 ml H2O). $FeCl_2$ $4H_2O$ (6.03 g in 75 ml H_2O) and $FeCl_3$ $6H_2O$ (8.28 g in 75 ml H2O) added together as sources of Fe^{2+} and Fe^{3+} ions during the neutralization process. The ratio between the two iron ions was set to one and their amounts with respect to Ca^{2+} ions was adjusted so as to obtain Fe/Ca ~ 20 mol.%. The synthesis was carried out in a heating mantle set at 45 °C and the temperature was controlled by means of a thermometer placed in the reacting solution. Once the dropwise addition of phosphoric acid was completed, the solution was kept at 45°C under constant stirring at 400 rpm for 3 hours and left ageing at room temperature overnight. ^{Fe}CaPs were recovered by centrifugation and extensively rinsed with water.

4. Physico-chemical characterization and stability

These activities are included in our recent publication (Adamiano et al. Inorganic Chemistry, 2017; Adamiano et al. Acta Biomaterialia, 2018). In figure 1a and figure 1b, a representative transmission electron microscopy (TEM) micrograph of ^{Fe}CaP-001 and its hydrodynamic diameter (Hd) size-distributions at nanoparticles concentrations corresponding to 1 mg/mL of Fe determined by dynamic light scattering (DLS) are respectively reported. ^{Fe}CaP-001 consists of (i) small isometric crystals of about 5–10 nm aggregated in needle-like nanoparticles having a length of 70-100 nm and width of 15-20 nm, and (ii) “dark spots” on the surface of needle-like ones corresponding to round-shaped electron dense nanoparticles with a diameter in the 5-15 nm size range. As previously reported, these “dark spots” are maghemite nanoparticles whose formation as secondary phase is due to the combination of two mechanisms occurring during ^{Fe}Cap-001 synthesis: (i) Fe^{2+} oxidation, and (ii) oxidation of magnetite formed by co-precipitation. ^{Fe}CaP-001 in HEPES buffer at pH 7.4 has a negative zeta potential of -44.1 ± 0.9 mV, and the relative Hd size-distributions has a zeta-average of 179.1 ± 3.2 nm.

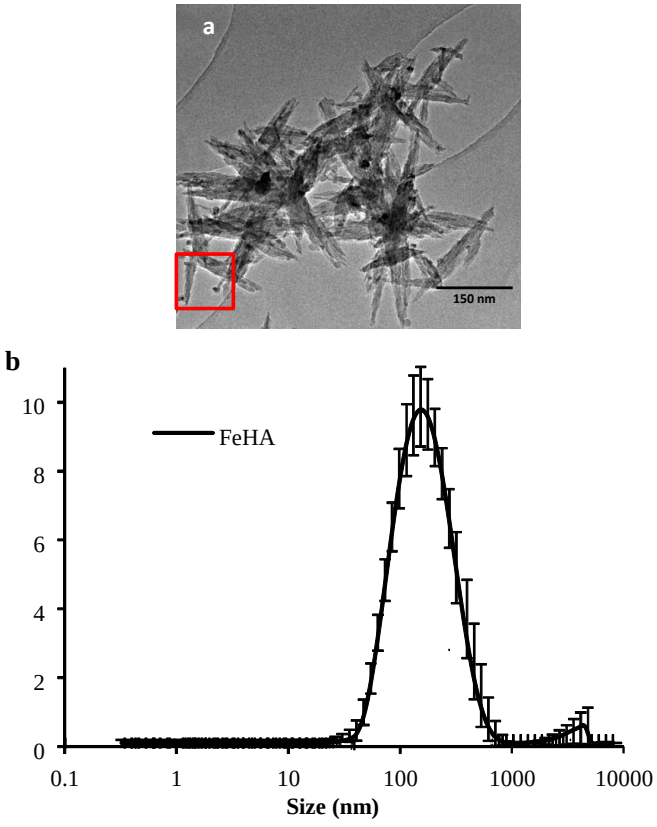

Figure 1. (a) TEM images and (b) DLS measurement (at physiological pH) of FeCaP (from Adamiano et al. Acta Biomaterialia, 2018).

To assess ^{Fe}CaP stability, suspensions of nanoparticles (NPs) (0.67 mg ml^{-1}) loaded with an amount of ibuprofen (IBU) (0.2 mg per mg of NPs) were injected into a fluidic circuit of citrate buffer (0.1 M, pH 6.0) (total volume = 5 ml) and HEPES buffer (0.01M, pH 7.4) under fluidic stimulations, this latter mimicking the cardiovascular environment (velocity of the flow = 5.7 cms^{-1}). After 5 and 120 minutes of flowing, the circulating solution was collected and absorbance readings at 266 nm were assessed spectrophotometrically to determine the amount of IBU. The chemical degradation of ^{Fe}CaPs, as well as CaPs used as reference, was evaluated under the same experimental conditions as the extent of Ca, P and Fe released in the flowing solution. Quantification was carried out by an inductively coupled plasma atomic emission (ICP-OES) spectrometer (Synchronous Vertical Dual View (SVDV) 5100, Agilent Technologies, US). Supernatants were collected after 2 hours under fluidic and magnetic stimulations and were dissolved in 1 wt.% ultrapure nitric acid. The analytical emission wavelengths were: Ca 422.673 nm, P 213.618 nm, and Fe 259.940 nm. Each measure has been recorded three times for statistical reliability. Notably, a higher IBU release was recorded from CaPs respect to ^{Fe}CaPs when exposed to fluid flow (not shown here). This effect is probably due to the higher affinity of IBU for ^{Fe}CaPs than CaPs, as evaluated by studying the adsorption kinetics and adsorption isotherms and their fitting according to the Sips model (Marrella et al. Journal of The Royal Society Interface, 2018).

The amounts of Ca, P and Fe released from ^{Fe}CaPs under fluidic conditions in HEPES buffer at physiological pH are reported in Figure 2. The control was measured in absence of flow. The data suggest a faster degradation of nanoparticles at increasing flow velocity, that in turn will lead to a faster release of the payload.

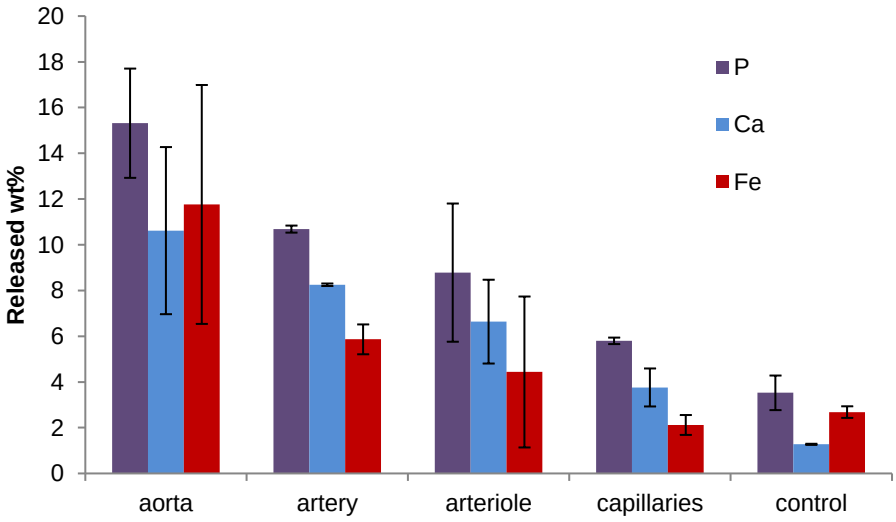

Figure 2. Stability test on ^{Fe}CaP-001 under different fluidic conditions simulating physiological conditions after 5 minutes. Results are expressed as the wt% of released elements from the nanoparticles. Error bars represent the standard deviation calculated on n=3 replicates. Info related to relations among vessel size and blood flow can be found here.

The same experiment performed in an acidic buffer gave different results, as reported in Figure 3. In this case, the flow velocity did not exert any significant effect on the degradation rate of NPs, that however was much faster for any tested flow velocity with respect to the control (no flow). This fact suggest that the simple presence/absence of the flow, independently from its velocity and even in acidic conditions (i.e. in an environment already boosting the carrier dissolution), affects the dissolution of the carrier, that in turn will lead to a quicker release of the payload.

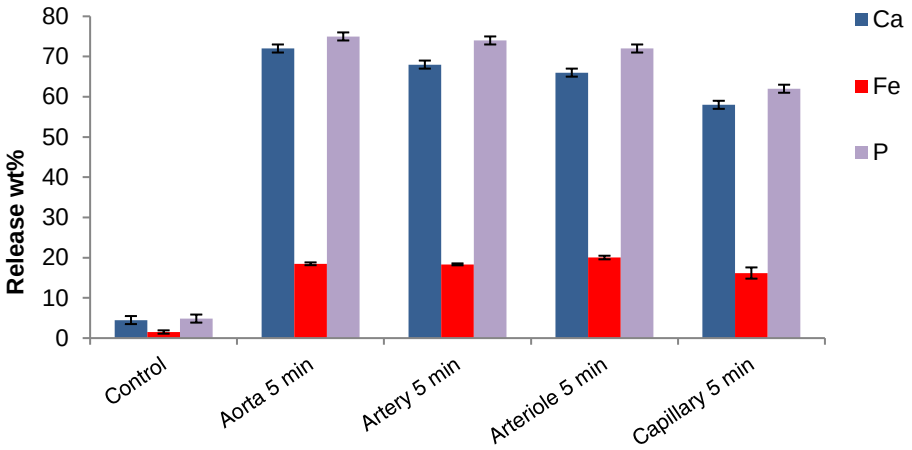

Figure 3. Stability test on ^{Fe}CaPs under different fluidic conditions in acidic buffer (pH 5.5) after 5 minutes. The results are expressed as the wt% of released elements from the nanoparticles. Error bars represent the standard deviation calculated on n=3 replicates.

5. Drug release tests

These activities are included in our recent publication (Marrella et al., J R Soc Interface. 2018).

The capability of ^{Fe}CaP-IBU to release the drug was assessed in function of the electromagnetic stimulation (EMF) applied. IBU was chosen as model drug thanks to its distinct spectrophotometric properties that facilitates the monitoring of the release. A fluidic circuit was placed inside a custom-made electro-magnetic stimulation apparatus and the efficacy of drug release was tested at different regimes of EMF, varying the frequencies of magnetic stimulation (15 Hz, 75 Hz, 100 Hz).

^{Fe}CaP and CaP (0.67 mg ml^{-1}) loaded with an amount of IBU 0.2 mg per mg of NPs were injected into a fluidic circuit of citrate buffer (0.1 M, pH 6.0) mimicking the acidic compartment of endosomes, and under coupled magnetic and fluidic stimulations, mimicking the cardiovascular environment (velocity of the flow = 5.7 cms-1). After 5 and 120 minutes of flowing, the circulating solution was collected and its absorbance readings at 266 nm was assessed by UV-Vis spectroscopy to determine the amount of IBU.

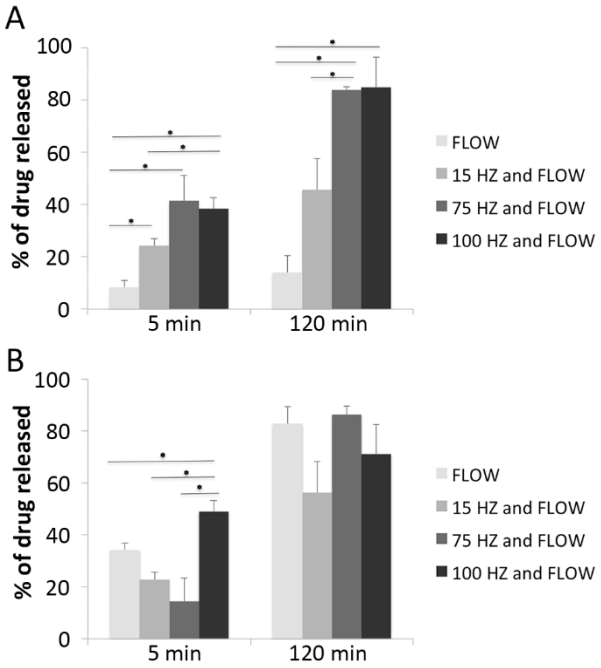

Figure 4. Percentage of IBU released within the fluidic circuit under magnetic and fluidic stimulation from ^{Fe}CaP (A) and CaPs (B) nanoparticles at different time points. Values are reported as mean ± SD, * indicates $p<0.05$ significance.

As shown in Figure 4, the application of a pulsed EMF on ^{Fe}CaP suspension improved the efficacy of drug release, which was proportional to the frequency of the applied EMF. The same experiments performed with CaP suspension gave no evidence on the occurrence of EMF induced release of IBU from the nanocarrier (Figure 4, Panel B).

A higher IBU release was recorded from CaPs respect to ^{Fe}CaPs when exposed to fluid flow stimulation. This effect is probably due to the lower affinity of IBU for CaP than ^{Fe}CaP as evaluated by studying the adsorption kinetics and adsorption isotherms and their fitting according to the Sips model.

To deepen the mechanisms of drug release from ^{Fe}CaP, the temperature increase during the electromagnetic stimulations was measured with an infrared thermo-camera. No temperature variations were observed, thus excluding any events of ^{Fe}CaP dissolution and hyperthermia effect from the mechanisms responsible of the magnetically triggered drug release. This conversely can be explained by a faster mechanical movement/vibration (i.e. shaking and flipping) of ^{Fe}CaPs at higher frequency of the EMF, prompting the detachment of ibuprofen molecules from their surface.

6. dp^{Fe}CaP generation and restoration

^{Fe}CaPs were transformed by spray-drying into dry powder of microparticles (dp^{Fe}CaPs). ^{Fe}CaPs were prepared by CNR-ISTEC at nominal concentrations of 10 mg/mL and transferred to PLU. The ^{Fe}CaP suspension has been diluted to 0.5 mg/ml ^{Fe}CaPs and transformed in respirable microparticles (aerodynamic size lower than 5 µm) by loading/dispersing the ^{Fe}CaPs in the soluble carrier mannitol, selected to produce the dry powders for inhalation. The procedure was carried out following the same optimized condition set in D1.1 for dpCaP generation. Two different conditions were tested producing dp^{Fe}CaPs with a ^{Fe}CaP: mannitol ratio of 1:2 and 1:4 ratio. dp^{Fe}CaPs produced presented a spherical shape, a morphology typical of mannitol spray dried particles and a size interval between 1 to 5 microns (Figure 5). This result denotes that, even when in small amount, the mannitol can drive the formation of spherical microparticles, in which the nanoparticles located at the surface creating a porous and less dense structure.

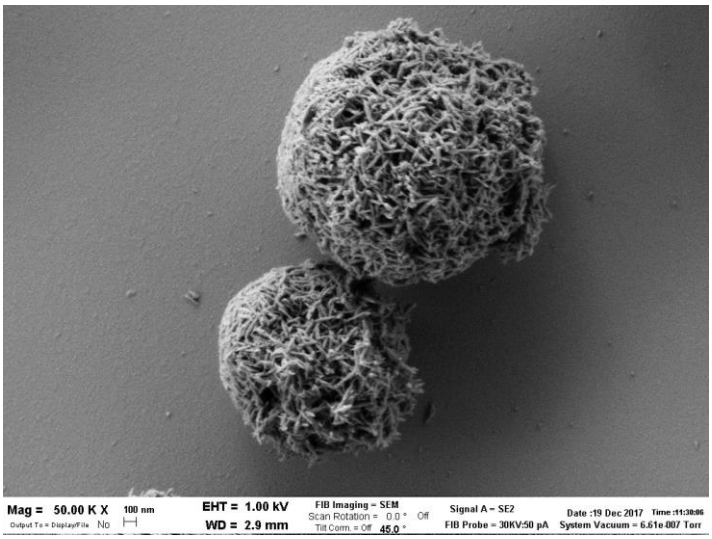

Figure 5. SEM image of dp^{Fe}CaPs produced with a ^{Fe}CaP : mannitol ratio 1:4.

The transformation of ^{Fe}CaPs in dp^{Fe}CaPs in the adopted spray drying conditions, highlighted the important effect of mannitol on the dispersion stability in term of size and aggregation of ^{Fe}CaPs (Figure 6).

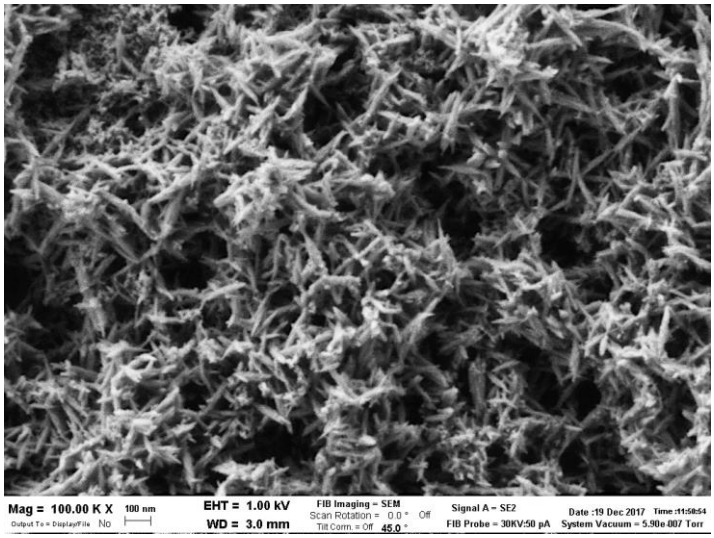

Figure 6. SEM image of dp^{Fe}CaPs after restoration.

7. ^{Fe}CaP restoration and drug release: *in vitro* functional assessment

The data relative to ^{Fe}CaPs and obtained from the restoration of CaPs from the dp^{Fe}CaPs are summarized in Table 1.

Table 1. Dimensional analysis of ^{Fe}CaPs and restored ^{Fe}CaPs.

	Z-AVERAGE (nm)	PDI	ZETA POTENTIAL (mV)
^{Fe}CaPs	191.2	0.2	-35.3
Restored ^{Fe}CaPs 1:2	190	0.2	-22
Restored ^{Fe}CaPs 1:4	144	0.2	-27

To evaluate the effect of different ^{Fe}CaP: mannitol ratios on the aggregation induced by the spray dryer procedure, the restoration protocol was carried out. dp^{Fe}CaPs dissolved in water show a size larger than the non-magnetic CaPs. These results shown that the size of ^{Fe}CaPs, both before the spray dry procedure and after microparticles restoration, are approximately double compared to CaPs. Additionally, the higher amount of mannitol employed for the generation of this dp^{Fe}CaPs partially prevented the aggregation of ^{Fe}CaPs and allowed for a better restoration of the nanoparticles in water.

The data reported on dp^{Fe}CaP morphology and size, and on ^{Fe}CaP restoration, colloidal stability and zeta potential, satisfactorily comply with our needs. Evaluations of nanoparticle interaction to cells are currently ongoing.

8. Conclusions

The performed activities support the proper generation of ^{Fe}CaPs, which are chemically and physically compatible with mannitol for their transformation into dp^{Fe}CaP microparticles. Effective modulation of drug release was confirmed in assays in function of the applied electromagnetic stimulation.